Turkish Journal of Electrical Engineering & Computer Sciences

http://journals.tubitak.gov.tr/elektrik/

Research Article

Turk J Elec Eng & Comp Sci
(2019) 27: 4246 – 4255

doi:10.3906/elk-1903-75

A novel randomized recurrent artificial neural network approach: recurrent random vector functional link network

Ömer Faruk ERTUĞRUL*
Department of Electrical and Electronics Engineering, Faculty of Engineering and Architecture, Batman University, Batman, Turkey

Received: 11.03.2019 • **Accepted/Published Online:** 25.07.2019 • **Final Version:** 26.11.2019

Abstract: The random vector functional link (RVFL) has successfully been employed in many applications since 1989. RVFL has a single hidden layer feedforward structure that also has direct links between the input layer and the output layer. Although nonlinearity, high generalization capacity, and fast training ability can be provided in RVFL, it can be found from the literature that higher nonlinearity can be obtained by adding recurrent feedback to an artificial neural network. In this paper, the recurrent type of RVFL (R-RVFL), which has both outer feedbacks and also inner feedbacks, is proposed. In order to evaluate and validate the proposed approach, a total of 109 public datasets were employed. Obtained results showed that R-RVFL can be employed successfully in terms of obtained success rates.

Key words: Recurrent random vector functional link, random vector functional link, inner feedback, outer feedback

1. Introduction

Artificial neural networks (ANNs) have been employed since 1943 [1] and, to date, many different types of ANNs (e.g., gradient-based methods and randomized methods) have been proposed. Determining optimum weights and biases by gradient-based methods (e.g., backpropagation) takes time by tuning, because of the large number of free parameters in the network. On the other hand, in randomized ones, some of these free parameters are assigned randomly and the others are calculated analytically. Therefore, randomized ones have high training speed and generalization capacity [2–4].

The random weight neural network (RNN), which is a randomized ANN, was proposed in 1992 by Schmidt et al. [5]. The random vector functional link network (RVFL), which is another randomized ANN, has a more general structure [6, 7]. In RVFL, in addition to a traditional feedforward ANN that has a single hidden layer, there are direct links between inputs and outputs that enhance the accuracy [2, 3]. In each of these methods, the weights and biases are assigned randomly and the other parameters, which are weights and biases in the output layer, are calculated analytically.

The literature findings showed that higher accuracies can be obtained by recurrent forms of an ANN model compared to their feedforward forms. The feedback connections were reported as one of the major reasons behind this higher success. It was expressed that the feedback connections provide a higher ability in modeling dynamic systems and enhanced the nonlinearity of the method because these connections act as a dynamic memory [8–13].

*Correspondence: omerfarukertugrul@gmail.com

The motivation behind this paper is to improve RVFL in order to have a recurrent form. The proposed recurrent RVFL (R-RVFL) was tested by 109 datasets that can be grouped as classification (31 datasets), regression (31 datasets), and time series (47 datasets) datasets. The obtained success rates showed that the proposed approach can be employed in classification and regression tasks. The rest of the paper is organized as follows. The list of employed benchmark datasets and their sources, the proposed approach, and the applied procedure are presented in Section 2. Obtained results are given and discussed in Section 3. Finally, Section 4 concludes this study.

2. Method

2.1. Traditional random vector functional links network

The structure of the RVFL artificial neural network is shown in Figure 1 [3].

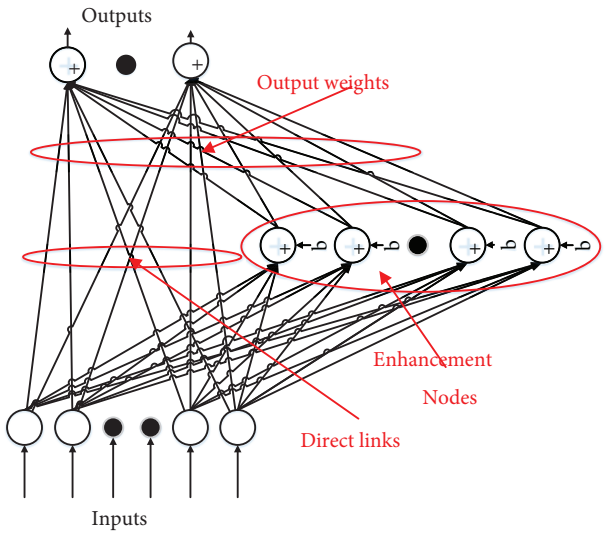

Figure 1. General structure of basic form of RVFL.

As seen in Figure 1, the output of RVFL is a summation of direct links from inputs and nonlinearly mapped inputs. The output of RVFL, y, can be calculated as follows:

$$y = \sum_{j=1}^{n} \beta_j x_j + \sum_{j=n+1}^{n+m} \beta_j g\left(\sum_{i=1}^{n} a_{i,j} x_i + b_j\right). \tag{1}$$

Here, x, n, m, $g()$, $a_{i,j}$, β_j, and b_j are the input, number of attributes, number of enhancement nodes, activation function (any piece of a differentiable function), weights in the hidden layer, weights in the output layer, and biases in the enhancement nodes and in the output layer, respectively. In RVFL, the weights in the hidden layer and biases in the enhancement nodes are assigned randomly. Therefore, the output of the jth enhancement node can be calculated by the following equation:

$$O_j = g\left(\sum_{i=1}^{n} a_{i,j} x_i + b_j\right). \tag{2}$$

Finally, the weights and biases in the output layer are calculated by Moore–Penrose pseudoinverse or ridge regression [3].

2.2. Novel proposed recurrent random vector functional links network

In R-RVFL, inner and outer feedbacks were added to the structure of RVFL as seen in Figure 2.

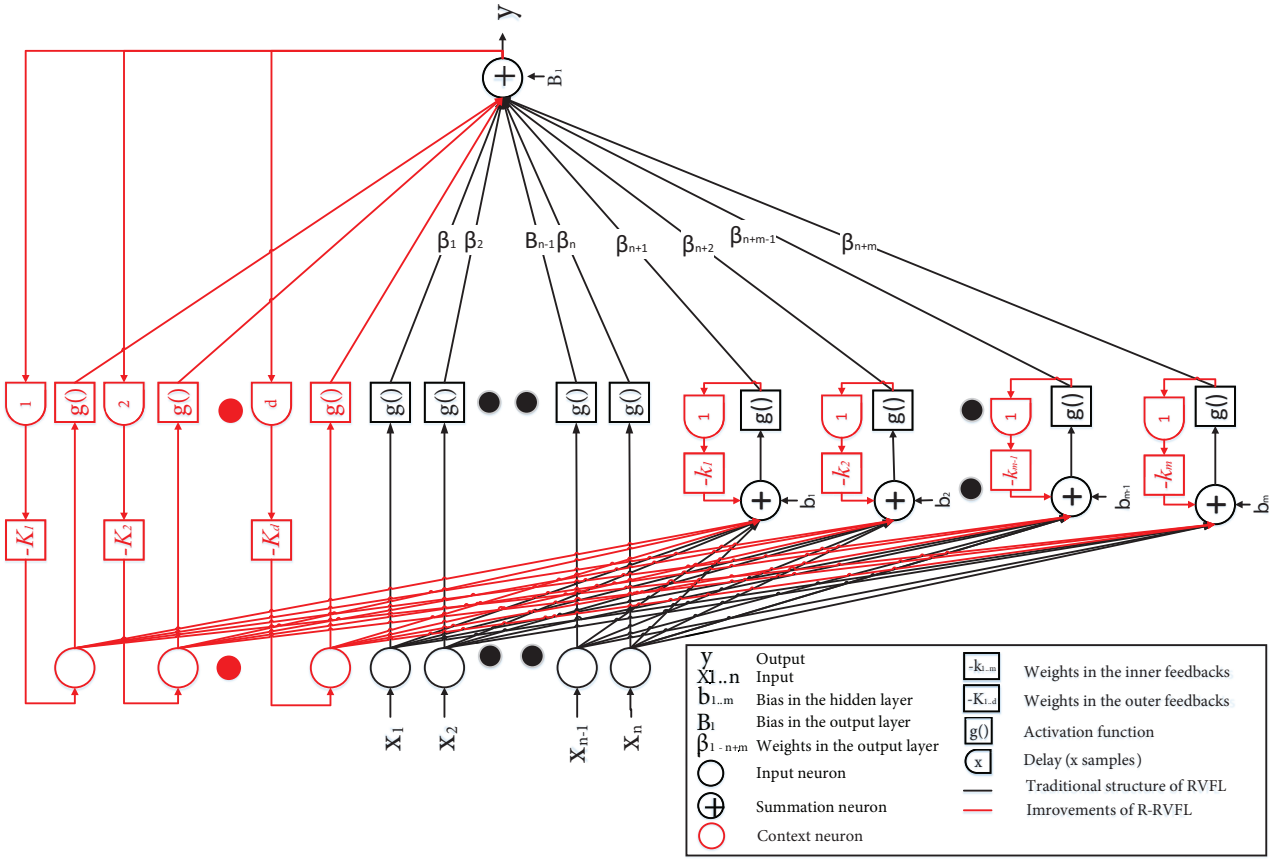

Figure 2. The structure of R-RVFL.

In R-RVFL, in addition to the weights in the hidden layer and the biases in the enhancement nodes, weights in the inner (k) and outer (K) feedbacks are also assigned arbitrarily. The output of R-RVFL (y^s) can be calculated as follows (see Figure 2):

$$y^s = \sum_{j=1}^{n} \beta_j x_j^s + \sum_{j=1}^{l} K_j x_j^{s-j} + \sum_{j=1}^{m} \beta_j \left\{ g\left(\sum_{i=1}^{n} a_{i,j} x_i^s + b_j \right) - k_j \beta_j g\left(\sum_{i=1}^{n} a_{i,j} x_i^{s-1} + b_j \right) \right\}, \tag{3}$$

where l, k, and K are the number of outer feedback connections and the inner and outer feedbacks weights, respectively. The calculations can be done sequentially and the output of each enhancement node of the sample s is updated according to the previous output of that enhancement node as follows:

$$O_j^s = g\left(\sum_{i=1}^{n} a_{i,j} x_i + b_j - k_j O_j^{s-1} \right). \tag{4}$$

Furthermore, as seen in Figure 2, context neurons were added to the structure of the RVFL network. The input of each context neuron was associated with a specific delay of the whole output of the RVFL according

to the weight of that outer feedback. These context neurons act similarly to other input neurons. Moreover, in traditional RVFL, there is not any activation function on the direct links and also bias in the output layer. In this version of RVFL, as seen in Figure 2, activation functions were also employed on direct links.

2.3. Applied methodology

In this study, the results achieved by the proposed R-RVFL were compared with the results obtained by an ANN that was trained by backpropagation, RNN, and RVFL. The applied methodology in this study can be summarized in three steps.

1st step: Normalizing the employed dataset into the range of –1 to 1.

2nd step: Determining the optimal network parameters. The parameters used in the trials are given in Table 1. The parameters were selected according to the achieved highest mean test success rate in cross-validation.

Table 1. Used parameters in the trials.

Parameter	Used in trials	Methods
Number of neurons in the hidden layer	5, 10, 15, 20, 30, 40, and 50	ANN, RNN, RVFL, and R-RVFL
Activation function	Sigmoid, sine, triangular basis, and radial basis	ANN, RNN, RVFL, and R-RVFL
Number of context neurons	0, 1, 2, 3, and 4 instances (samples)	R-RVFL

Accuracy and root mean square error (RMSE) were used as success rates in classification and regression datasets, respectively. These validation metrics are calculated as follows:

$$Accuracy\,(\%) = 100 * \frac{\#Trueclassifiedsamples}{\#Allsamples}\%, \tag{5}$$

$$RMSE = \sqrt{\frac{1}{N}\sum_{i=1}^{N}(f_i - y_i)^2}, \tag{6}$$

where f, y, and N are the desired value, obtained value, and number of observations (samples) in the dataset, respectively.

3rd step: Employing the ANN, RNN, RVFL, and R-RVFL in each dataset. Two different test procedures were employed. The first one is 5-fold cross-validation and all classification, regression, and time series datasets were classified/estimated according to 5-fold cross-validation [14]. The second procedure is Monte Carlo cross-validation and only time series datasets were employed in this procedure according to the following training-test partitions [15] (see Table 2). Based on the applied procedures, the same data partitions were used in each employed method.

2.4. Utilized datasets

In order to validate the proposed approach, 109 benchmark datasets were employed. The datasets can be divided into 3 groups as follows.

Table 2. Used partitions in Monte Carlo cross-validation.

Partition #	Training partition	Test partition
1	First 40% of the dataset	Next 4% of the dataset
2	First 50% of the dataset	Next 5% of the dataset
3	First 60% of the dataset	Next 6% of the dataset
4	First 70% of the dataset	Next 7% of the dataset
5	First 80% of the dataset	Next 8% of the dataset

a) Employed classification datasets (31 datasets): Lithuanian [16], Highleyman [16], banana shaped [16], spherical [16], multiclass [16], liver,[1] Pima Indian diabetes,[1] hepatitis,[1] image segmentation,[1] satellite image,[1] statlog (shuttle),[1] abalone,[1] wine,[1] breast tissue,[1] cardiotocography,[1] skin segmentation,[1] seeds,[1] EEG eye state,[1] seismic bumps,[1] banknote authentication,[1] balance scale,[1] acute inflammations,[1] dermatology,[1] diabetic retinopathy Debrecen,[1] fertility,[1] glass,[1] Haberman,[1] Hayes-Roth,[1] QSAR biodegradation,[1] climate,[1] and banana[2] datasets.

b) Employed regression datasets (31 datasets): approximate sinc [16], forest fire,[1] CASP 5-9,[1] İstanbul stock exchange,[1] auto-price,[1] Boston housing,[1] servo,[1] breast cancer,[1] CPU-small,[1] CPU,[1] machine-CPU,[1] energy efficiency: cooling,[1] energy efficiency: heating,[1] yacht, [1] diabetes child,[3] delta elevators,[3] elevators,[3] kinematics,[3] puma-8NH,[3] puma-32H,[3] pyrimidines,[3] stocks,[3] triazines,[3] bank-8FM,[3] ailerons,[3] delta ailerons,[3] California housing,[3] census-8L,[3] census-8H,[3] census-16L,[3] and census-16H.[3]

c) Time regression datasets (47 datasets): solar station ID: 722255,[4] solar station ID: 722700,[4] solar station ID: 744860,[4] solar station ID: 911900,[4] MSL station ID: 1111,[5] MSL station ID: 1391,[5] MSL station ID: 1673,[5] MSL station ID: 2093,[5] MSL station ID: 2171,[5] MSL station ID: 638,[5] MSL station ID: 913,[5] S& P 500 futures,[6] NQ 100 futures,[6] Dow 30,[6] Russell 2000,[6] DAX,[6] CAC 40,[6] FTSE 100,[6] DJ Euro Stoxx 50,[6] FTSE MIB,[6] SMI,[6] IBEX 35,[6] WIG20,[6] BUX,[6] OBX,[6] iBovespa,[6] IPC,[6] BIST 30,[6] Hang Sengs,[6] China H-Shares,[6] Singapore MSCI,[6] BSE Sensex 30,[6] NITFY,[6] KOSPI 200,[6] Nikkei 225,[6] US Dollar index,[6] EUR/USD,[6] US 30Y T-Bond,[6] Euro Bund,[6] Japan Govt. Bond,[6] crude oil,[6] natural gas,[6] gold,[6] copper,[6] and US-wheat.[6]

3. Results and discussion

In this section, first, the effect of the parameters of the R-RVFL will be investigated. Later, results achieved by R-RVFL will be compared with results obtained by ANN, RNN, and RVFL.

[1]UCI Machine Learning Repository (2019) [online]. Website: http://archive.ics.uci.edu/ml [accessed 28 08 2019].
[2]MLDATA (2019) [online]. Website: http://mldata.org/repository/data/viewslug/banana-ida/ [accessed 28 08 2019].
[3]DCC (2019) [online]. Website: http://www.dcc.fc.up.pt/∼ltorgo/Regression/DataSets.html [accessed 28 08 2019].
[4]NOAA (2019) [online]. Website: https://www.ncdc.noaa.gov/data-access/land-based-station-data/land-based-datasets/solar-radiation [accessed 28 08 2019].
[5]PSMSL (2019) [online]. Website: http://www.psmsl.org/ [accessed 28 08 2019].
[6]Investing (2019) [online]. Website: https://www.investing.com/ [accessed 28 08 2019].

3.1. Analysis of proposed approach

In order to analyze the properties of the proposed approach, the Lithuanian, forest fire, and Dow 30 datasets were used in tests and the effect of the parameters of R-RVFL was assessed according to obtained mean accuracies in cross-validations. First, R-RVFL was assessed according to the inner and outer feedbacks and obtained mean accuracies are summarized in Table 3. Note that the datasets marked with an asterisk were estimated according to Monte Carlo cross-validation based on the orders of the samples, while the others were classified/estimated according to 5-fold cross-validation.

Table 3. Effect of inner and outer feedbacks on the obtained accuracy.

Dataset	Inner feedback: $\surd$ Outer feedback: $\surd$	Inner feedback: $\surd$ Outer feedback: X	Inner feedback: X Outer feedback: $\surd$	Inner feedback: X Outer feedback: X
Lithuanian (%)	99.90	99.50	99.80	96.00
Forest fire	0.0469	0.0493	0.0471	0.0477
Dow 30	0.0087	0.1457	0.0089	0.1456
Dow 30$*$	0.0057	0.1122	0.0278	0.1122

As seen in Table 3, in the Lithuanian dataset, the inner feedbacks are as important as the outer feedbacks. On the other hand, in the forest fire dataset, Dow 30, and Dow 30$*$ datasets, it can be said that the proposed approach does not gain any extra knowledge in inner feedbacks (i.e. there is not any requirement of inner feedback). However, the findings given in Table 3 show that using both inner and outer feedbacks boosts the overall success and is the main difference between the structure of RVFL. This may be explained by the features of the cascaded control scheme [17], since the disturbances can be eliminated faster, the controllability of the inputs is increased, and time delay effects are reduced [18]. Furthermore, the obtained success rates are related to the number of context neurons, which is the same as the number of outer feedbacks, as summarized in Table 4.

Table 4. Effect of number of context neurons on the obtained accuracy.

Dataset	Number of context neurons								
	0	1	2	3	4	5	6	7	8
Lithuanian (%)	99.50	99.80	99.80	99.80	99.90	99.80	99.80	99.80	99.90
Forest fire	0.0473	0.0486	0.0491	0.0478	0.0469	0.0482	0.0600	0.0477	0.0634
Dow 30	0.1457	0.0095	0.0087	0.0087	0.0087	0.0089	0.0087	0.0085	0.0083
Dow 30$*$	0.1122	0.0057	0.0063	0.0057	0.0057	0.0057	0.0057	0.0057	0.0059

As seen in Table 4, a correlation between obtained success rates and the number of context neurons was not found. Therefore, these results show that the optimum number of context neurons must be determined by trials or maybe by an expert opinion. Furthermore, it can be said that for each of the employed datasets, using context neurons increases the success in terms of accuracy, but the increase in the number of used context neurons did not yield an increase in accuracy. It can be said that the number of context neurons may depend on the characteristics of the dataset. Moreover, the effect of output bias, direct link, and activation function in the direct link was tested and obtained success rates are given in Table 5.

As seen in Table 5, the output bias does not boost the success rate in the employed datasets. On the

Table 5. Effect of output bias, direct link, and activation function on the obtained accuracy.

Dataset	Output bias: √ Direct link: √ Activation f.: √	Output bias: √ Direct link: √ Activation f.: X	Output bias: √ Direct link: X Activation f.: X	Output bias: X Direct link: √ Activation f.: √	Output bias: X Direct link: X Activation f.: X
Lithuanian (%)	99.90	99.90	99.90	99.90	99.90
Forest fire	0.0469	0.0481	0.0458	0.0549	0.458
Dow 30	0.0087	0.0088	0.0109	0.0088	0.0099
Dow 30∗	0.0057	0.0087	0.0155	0.0057	0.1505

other hand, using an activation function in the direct link increases the success of the RVFL. Moreover, having a direct link and the activation in the network structure increases the success of the R-RVFL. Consequently, reported results in Table 5 suggest that the direct link and the activation function in the direct link boost the success of R-RVFL. This result supports the finding of Zhang and Suganthan that direct links have a high impact on the increase of the success of the RVFL [3]. Although a boosting effect of the output bias was not observed, using output bias did not yield a decrease in the success of the proposed approach.

3.2. Obtained general results

Before starting validation of R-RVFL, the parameters of ANN, RNN, RVFL, and R-RVFL were determined by trials and the optimum parameters were determined based on obtained test success rates. The obtained RMSEs for the forest fire dataset by RNN (the same parameters were obtained by ANN), RVFL, and R-RVFL are shown in Figure 3 as an example (note that # CN in Figure 3 refers to number of the context neurons). As seen in Figure 3, the obtained RMSEs were highly dependent on the structure of the network. Furthermore, in the ANN, RNN, and RVFL, determining the optimum number of neurons in the hidden layer and the optimal activation function is required. However, in R-RVFL, in addition to the number of neurons in the hidden layer and the activation function, the number of context neurons must be optimized. Therefore, the number of required trials in the optimization of R-RVFL is higher than in ANN, RNN, and RVFL, but still the number of parameters that must be optimized in R-RVFL, similar to both of the other employed RNN and RVFL methods, is less than the parameters in the ANN that was trained by backpropagation, which is a gradient-based method (e.g., learning rate, number of maximum epochs, stopping criteria) [2, 3]. After optimization of each employed method, each particular dataset was classified/estimated based on cross-validation strategies. Obtained success rates for each dataset are reported in the Appendix (see Tables A1–A4) and obtained mean success rates are reported in Table 6.

Table 6. Obtained mean success rates.

Datasets	Training accuracy / RMSE				Test accuracy / RMSE			
	ANN	RNN	RVFL	R-RVFL	ANN	RNN	RVFL	R-RVFL
Classification (%)	87.60	87.51	81.88	91.66	77.12	77.54	70.15	84.99
Regression	0.1092	0.1106	0.1259	0.0992	0.1257	0.1239	0.1216	0.1121
Time series	0.0899	0.0898	0.0988	0.0619	0.0977	0.0977	0.0910	0.0131
Time series*	0.0813	0.0812	0.0902	0.0437	0.0884	0.0883	0.0829	0.0098

As seen in Table 6, the achieved mean success rates by R-RVFL are higher than the obtained success rates by other employed methods. Furthermore, lower mean RMSE was obtained in estimating in time series datasets according to the orders of the samples and this result supports the literature findings [10, 11, 19]. Consequently, as seen in this table, higher success rates were obtained by the recurrent form of the RVFL (R-RVFL) compared with RVFL. The main reason for this success is explained by feedback connections [10, 11]. These feedback connections (i.e. context neurons, delays) proceed as dynamic memory [8], and this dynamic memory yields a higher modeling capability [8, 9, 12]. Additionally, it was stated by Alanis et al. that because of this property even difference equations that could not be modeled by feedforward ANNs can be modeled [12]. Furthermore, in [13], it was reported that recurrent links enhance the ability of mapping nonlinear dynamics and especially modeling nonlinear real-time variables. In order to investigate optimized network complexities, the mean number of neurons in the hidden layer, mean number of context neurons, and most common (mode) activation functions are given in Table 7.

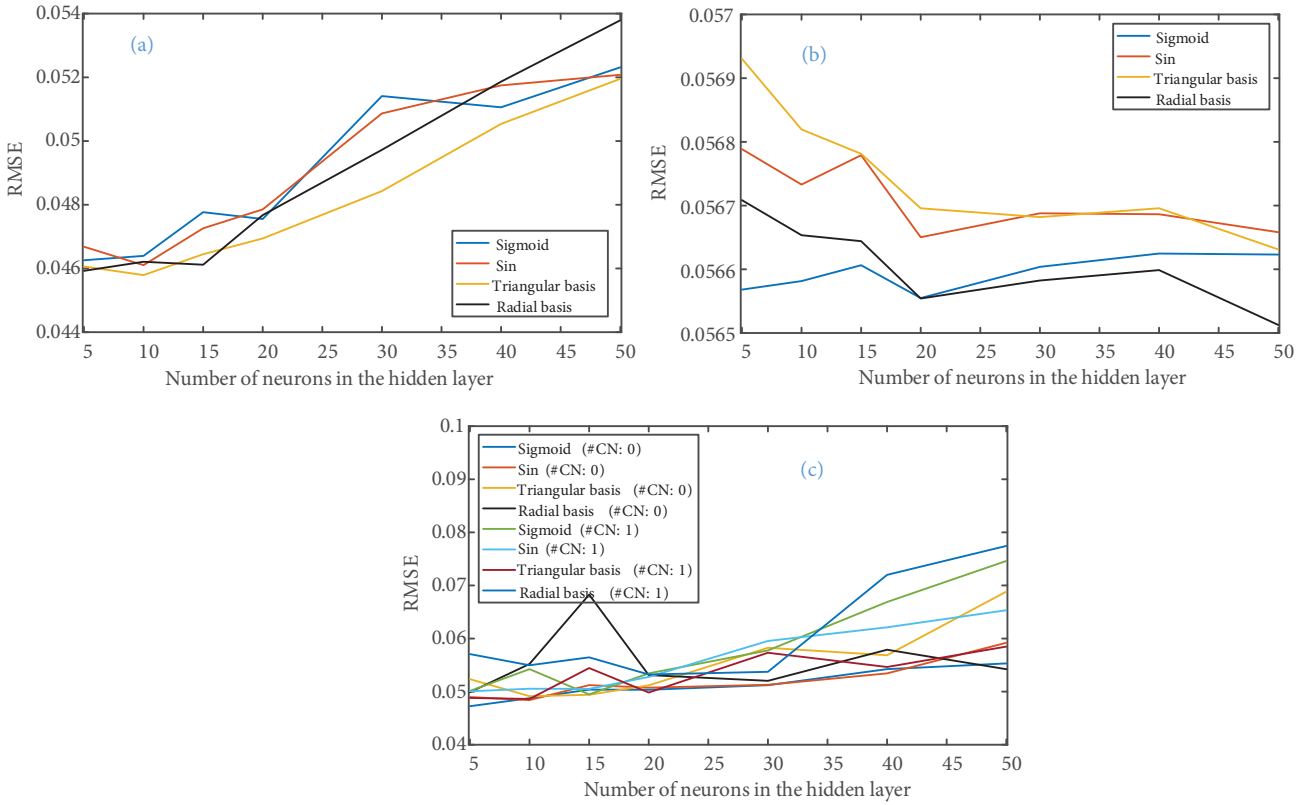

Figure 3. Determining optimal parameters in: (a) RNN, (b) RVFL, and (c) R-RVFL.

As seen in Table 7, the mean of the required number of neurons in the hidden layer by R-RVFL is lower than the required number of neurons in the hidden layer by other employed methods. Furthermore, a correlation between optimum activation function and the employed method could not be found. Additionally, the computational costs of R-RVFL and other employed methods are given in Table 8 in terms of mean process time (s).

Although it can be seen in Table 8 that the means of the required number of neurons in the hidden layer are lower than in the other methods, processing times in both training and test stages by RVFL are higher

than in the other employed methods. The reason for this is the sequential computation algorithm of R-RVFL, which is because of the recurrent links. Furthermore, as explained before, an extra number of trials is required in order to optimize R-RVFL. Even though R-RVFL requires higher processing time, the computational cost of R-RVFL is still in an acceptable range based on obtained results by ANN (see Table 8). The reason for this is explained in the literature as randomly assigning some parameters and analytically calculating others instead of optimizing them by tuning (e.g., backpropagation, Levenberg–Marquardt methods) [4].

Table 7. Optimized parameters in employed methods.

Datasets	#Neurons in the hidden layer				#Context neurons	Activation function			
	ANN	RNN	RVFL	R-RVFL		ANN	RNN	RVFL	R-RVFL
Classification	30.32	35.16	26.77	24.03	1.77	Sigmoid	Sigmoid	Sigmoid	Sigmoid
Regression	32.74	36.45	34.35	31.29	1.68	Sigmoid	Sigmoid	Radial basis	Sin
Time series	24.33	25.78	37.67	6.78	2.31	Sigmoid	Sigmoid	Radial basis	Triangular basis
Time series*	15.78	13.11	45.89	6.56	2.64	Sigmoid	Sigmoid	Sigmoid	Triangular basis

Table 8. Mean process time (s).

Datasets	Training stage				Test stage			
	ANN	RNN	RVFL	R-RVFL	ANN	RNN	RVFL	R-RVFL
Classification	1.15	0.090	0.083	0.092	0.08	0.090	0.083	0.021
Regression	0.78	0.101	0.090	0.184	0.09	0.101	0.090	0.034
Time series	0.61	0.049	0.042	0.091	0.07	0.049	0.042	0.025
Time series*	0.45	0.021	0.023	0.038	0.03	0.021	0.023	0.004

4. Conclusion

According to the results obtained in this study, it can be said that the recurrent links boosted the network performance but on the other hand they also increased the computational cost. The reason for obtaining higher accuracies was addressed in the literature as the context neurons that can be associated with memory provide higher nonlinearity. Therefore, this yields an increase in the adaptability of the machine learning method, and in this way, even dynamic systems can be modeled. Furthermore, based on the relationship between the control systems and the machine learning methods, this study showed that higher accuracies can be obtained by a recurrent model based on cascaded control systems (using inner and outer feedbacks together) compared to traditional recurrent models that used only outer feedbacks.

References

[1] McCulloch WS, Pitts W. A logical calculus of the ideas immanent in nervous activity. Bulletin Of Mathematical Biophysics 1943; 5 (4): 115–133. doi: 10.1007/BF02478259

[2] Wang D. Editorial: Randomized algorithms for training neural networks. Information Sciences 2016; 364–365: 126–128. doi: 10.1016/j.ins.2016.12.007

[3] Zhang L, Suganthan PN. A comprehensive evaluation of random vector functional link networks. Information Sciences 2016; 367–368: 1094–1105. doi: 10.1016/j.ins.2015.09.025

[4] Zhang L, Suganthan PN. A survey of randomized algorithms for training neural networks. Information Sciences 2016; 364: 146–155. doi: 10.1016/j.ins.2016.01.039

[5] Schmidt WF, Kraaijveld MA, Duin RPW. Feed forward neural networks with random weights. In: IEEE 11th International Conference on Pattern Recognition; The Hague, the Netherlands; 1992. pp. 1–4.

[6] Pao YH, Park GH, Sobajic DJ. Learning and generalization characteristics of the random vector functional-link net. Neurocomputing 1994; 6 (2): 163–180. doi: 10.1016/0925-2312(94)90053-1

[7] Li M, Wang D. Insights into randomized algorithms for neural networks: practical issues and common pitfalls. Information Sciences 2017; 382–383: 170–178. doi: 10.1016/j.ins.2016.12.007

[8] Ho S, Xie M, Goh T. A comparative study of neural network and Box-Jenkins ARIMA modeling in time series prediction. Computers and Industrial Engineering 2002; 42 (2): 371–375. doi: 10.1016/S0360-8352(02)00036-0

[9] Lukoševičius M, Jaeger H. Reservoir computing approaches to recurrent neural network training. Computer Science Review 2009; 3 (3): 127–149. doi: 10.1016/j.cosrev.2009.03.005

[10] Kermanshahi B. Recurrent neural network for forecasting next 10 years loads of nine Japanese utilities. Neurocomputing 1998; 23 (1): 125–133. doi: 10.1016/S0925-2312(98)00073-3

[11] Pai PF, Hong WC. Forecasting regional electricity load based on recurrent support vector machines with genetic algorithms. Electric Power Systems Research 2005; 74 (3): 417–425. doi: 10.1016/j.epsr.2005.01.006

[12] Alanis AY, Sanchez EN, Loukianov AG, Hernandez EA. Discrete-time recurrent high order neural networks for nonlinear identification. Journal of the Franklin Institute 2010; 347 (7): 1253–1265. doi: 10.1016/j.jfranklin.2010.05.018

[13] Li L, Haykin S. A cascaded recurrent neural network for real-time nonlinear adaptive filtering. In: IEEE International Conference on Neural Networks; San Francisco, CA, USA; 1993. pp. 857–62. doi: 10.1109/ICNN.1993.298670

[14] Kohavi R. A study of cross-validation and bootstrap for accuracy estimation and model selection. In: International Joint Conference on Artificial Intelligence; Montreal, Canada; 1995. pp. 1–7.

[15] Xu QS, Liang YZ. Monte Carlo cross validation. Chemometrics and Intelligent Laboratory Systems 2001; 56 (1): 1–11. doi: 10.1016/S0169-7439(00)00122-2

[16] Duin RP, Juszczak P, Paclik P, Pekalska E, De Ridder D. PR-Tools 4.0, A MATLAB Toolbox for Pattern Recognition. The Netherlands, 2004.

[17] Arrieta O, Vilanova R, Balaguer P. Procedure for cascade control systems design: choice of suitable PID tunings. International Journal of Computers Communications and Control 2008; 3 (3): 235–248. doi: 10.15837/ijccc.2008.3.2392

[18] Shinskey FG. Process-Control Systems: Application, Design, Adjustment. New York, NY, USA: McGraw-Hill, 1979.

[19] Ertuğrul ÖF. A novel approach for extracting ideal exemplars by clustering for massive time-ordered datasets. Turkish Journal of Electrical Engineering and Computer Sciences 2017; 25 (4): 2614-2634. doi: 10.3906/elk-1602-341

Table A1. Obtained classification accuracies (%) and optimum network parameters.

Datasets	Training accuracy (%)				Test accuracy (%)				Optimum # hidden neurons				Delay
	RNN	RVFL	ANN	R-RVFL	RNN	RVFL	ANN	R-RVFL	RNN	RVFL	ANN	R-RVFL	
Lithuanian	97.08	96.65	96.83	99.78	95.50	95.30	95.40	99.90	40	20	5		4
Highleyman	92.48	87.13	93.08	99.95	88.70	76.50	88.90	99.90	50	50	50	20	1
Banana Shaped	98.75	92.08	98.75	99.78	98.20	87.40	98.00	99.80	50	10	50	5	1
Spherica	84.88	82.25	85.15	99.78	80.10	73.80	79.60	99.80	40	50	40	5	1
Multi-Class	92.55	77.50	92.00	98.85	40.70	20.30	39.50	45.50	50	50	50	50	1
Liver	75.24	71.59	73.39	72.19	71.11	71.62	71.28	70.77	40	30	20	15	0
Pima Indian Diabetes	81.01	77.04	78.66	81.01	78.83	76.62	76.75	78.70	50	10	30	30	0
Hepatitis	98.75	77.19	98.44	96.25	71.25	57.50	68.75	93.75	50	5	50	10	2
Banana	90.48	87.85	90.30	87.07	83.72	73.53	87.21	80.77	50	50	40	40	0
Image Segmentation	92.62	88.57	93.32	98.65	85.92	78.10	84.49	96.29	40	50	50	50	4
Satellite Image	85.06	77.60	85.06	90.43	83.90	76.85	83.92	88.97	50	50	50	50	1
Statlog (Shuttle)	99.38	93.59	97.28	97.82	99.35	93.58	97.25	97.80	50	40	50	50	2
Abalone	28.80	26.28	28.98	30.40	25.87	24.57	25.46	27.02	30	50	30	30	4
Wine	99.86	95.92	99.15	99.58	93.89	82.78	92.22	97.78	30	30	15	10	3
Breast tissue	80.47	65.88	80.47	93.88	13.33	0.95	9.52	27.62	20	5	20	20	2
Cardiotocography	94.27	91.30	93.32	95.90	92.89	90.07	91.29	93.74	50	5	40	50	3
Skin segmentation	98.92	98.67	99.06	100.00	84.74	78.01	84.47	100.00	50	40	50	5	1
Seeds	97.50	87.50	97.26	98.93	93.81	59.05	92.86	99.52	10	20	10	5	2
EEG eye state	57.71	57.06	60.76	99.84	46.63	38.95	39.49	99.84	5	10	10	15	1
Seismic Bumps	93.39	93.42	93.41	93.39	93.38	93.42	93.38	93.27	5	5	5	5	4
Banknote authentication	99.89	97.78	99.89	99.96	99.71	97.30	99.71	99.85	40	40	40	50	0
Balance Scale	91.68	89.80	90.08	91.24	90.88	88.00	88.16	89.92	30	50	10	50	3
Acute Inflammations	100.00	100.00	100.00	100.00	100.00	100.00	100.00	100.00	10	5	10	5	0
Dermatology	98.57	98.16	97.61	99.52	95.89	96.99	96.16	96.99	50	20	20	30	3
Diabetic Retinopathy	75.18	66.04	74.94	74.27	72.61	64.70	71.83	71.39	40	5	40	15	4
Fertility	88.00	88.00	88.00	88.00	88.00	88.00	88.00	88.00	5	5	5	5	0
Glass	76.02	59.65	85.73	96.02	26.05	9.77	29.30	59.53	20	10	50	30	3
Haberman	77.63	74.04	77.80	84.00	66.23	73.44	75.08	81.31	15	50	15	15	3
Hayes-Roth	87.74	64.15	88.87	82.64	73.08	46.15	74.62	65.38	30	50	30	20	1
QSAR biodegradation	86.78	84.17	86.66	99.57	77.44	70.05	76.59	99.62	50	10	50	5	1
Climate	92.08	91.48	91.48	92.64	92.04	91.48	91.48	92.04	40	5	5	50	3

Table A2. Obtained RMSEs in regression datasets and optimum network parameters.

Datasets	Training RMSE				Test RMSE				Optimum # hidden neurons				Delay
	RNN	RVFL	ANN	R-RVFL	RNN	RVFL	ANN	R-RVFL	RNN	RVFL	ANN	R-RVFL	
Approximate Sinc	0.5739	0.5744	0.5739	0.5737	0.5743	0.5739	0.5743	0.5741	5	40	5	5	0
Forest Fire	0.0568	0.0459	0.0569	0.0560	0.0452	0.0564	0.0456	0.0469	10	50	5	10	4
CASP 5-9	0.0390	0.0409	0.0387	0.0392	0.0392	0.0409	0.0392	0.0395	50	50	50	50	0
İstanbul Stock Exchange	0.1333	0.1382	0.1386	0.1281	0.1428	0.1369	0.1409	0.1354	15	5	10	10	1
Ailerons	0.0741	0.0767	0.0740	0.0737	0.0753	0.0761	0.0754	0.0756	40	50	40	50	2
Delta Ailerons	0.0002	0.0002	0.0002	0.0002	0.0002	0.0002	0.0002	0.0002	50	50	40	40	3
Auto-Price	0.0600	0.0998	0.0737	0.0460	0.1100	0.0916	0.0962	0.0756	20	10	10	10	2
Bank-8FM	0.0464	0.0496	0.0463	0.0445	0.0470	0.0495	0.0470	0.0452	50	5	50	50	0
Boston Housing	0.0641	0.1104	0.0864	0.0740	0.1357	0.1017	0.1151	0.1033	40	10	20	15	2
Breast Cancer	0.2605	0.2716	0.2456	0.2007	0.2874	0.2407	0.2805	0.2688	5	5	10	5	2
California Housing	0.1244	0.1508	0.1253	0.0942	0.1330	0.1455	0.1327	0.0961	50	50	40	50	3
Census-8L	0.0684	0.0773	0.0687	0.0715	0.0696	0.0772	0.0693	0.0720	50	50	40	40	0
Census-8H	0.0820	0.0897	0.0834	0.0841	0.0830	0.0896	0.0849	0.0851	50	50	50	50	1
Census-16L	0.0771	0.0826	0.0769	0.0767	0.0778	0.0824	0.0775	0.0775	50	50	50	50	0
Census-16H	0.0828	0.0879	0.0855	0.0850	0.0834	0.0878	0.0860	0.0856	50	40	50	50	0
CPU-Small	0.0398	0.0619	0.0419	0.0433	0.0422	0.0615	0.0464	0.0453	50	50	50	50	0
CPU	0.0540	0.0726	0.0741	0.0546	0.0557	0.0719	0.0779	0.0576	50	40	50	50	2
Diabetes Child	0.1594	0.0979	0.0882	0.0828	0.1991	0.0950	0.2351	0.0852	30	50	5	5	3
Delta Elevators	0.1095	0.1105	0.1101	0.1097	0.1104	0.1099	0.1107	0.1107	50	50	30	50	1
Elevators	0.0751	0.0767	0.0751	0.0248	0.0760	0.0765	0.0759	0.0252	50	50	50	50	4
Kinematics	0.1130	0.1175	0.1127	0.1168	0.1140	0.1168	0.1138	0.1181	50	30	50	50	4
Machine-CPU	0.0288	0.0645	0.0314	0.0261	0.0375	0.0544	0.0362	0.0434	15	5	10	20	4
Puma-8NH	0.3581	0.3620	0.3612	0.3555	0.3618	0.3599	0.3649	0.3588	50	50	50	40	0
Puma-32H	0.3011	0.3029	0.3012	0.2984	0.3041	0.2977	0.3045	0.3010	40	50	40	5	2
Pyrimidines	0.0977	0.0940	0.0582	0.0483	0.1192	0.0873	0.1145	0.1490	10	50	20	5	4
Servo	0.0685	0.1725	0.0604	0.0663	0.0916	0.1638	0.0931	0.1093	30	5	40	40	0
Stocks	0.0245	0.0697	0.0182	0.0215	0.0489	0.0375	0.0564	0.0138	20	10	30	5	4
Triazines	0.1311	0.1594	0.1305	0.1203	0.1627	0.1468	0.1610	0.1748	30	50	30	5	0
Energy Eff.: cooling	0.0635	0.0730	0.0629	0.0480	0.0650	0.0705	0.0655	0.0543	20	50	20	40	3
Energy Eff.: heating	0.0002	0.0146	0.0002	0.0000	0.0007	0.0142	0.0006	0.0000	50	5	50	20	0
Yacht	0.0617	0.1560	0.0857	0.0112	0.1493	0.1544	0.1759	0.0465	50	5	20	50	1

Table A3. Obtained RMSEs in time series datasets and optimum network parameters.

Datasets	Training RMSE				Test RMSE				Optimum # hidden neurons				Delay
	RNN	RVFL	ANN	R-RVFL	RNN	RVFL	ANN	R-RVFL	RNN	RVFL	ANN	R-RVFL	
SS. ID: 722255	0.1024	0.1090	0.1033	0.0224	0.1035	0.1080	0.1043	0.0232	50	30	50	20	1
SS. ID: 722700	0.1003	0.1086	0.1012	0.0176	0.1014	0.1076	0.1022	0.0213	50	30	50	30	1
SS. ID: 744860	0.1664	0.1668	0.1668	0.0620	0.1641	0.1690	0.1641	0.0537	50	50	10	20	3
SS. ID: 911900	0.0666	0.0803	0.0685	0.0178	0.0672	0.0799	0.0691	0.0178	50	50	40	20	3
MSL ID: 1111	0.0091	0.0117	0.0091	0.0251	0.0101	0.0108	0.0101	0.0064	15	50	20	5	2
MSL ID: 1391	0.0398	0.0451	0.0398	0.0369	0.0428	0.0425	0.0428	0.0326	10	15	40	5	3
MSL ID: 1673	0.0094	0.0157	0.0095	0.0412	0.0104	0.0150	0.0104	0.0085	15	50	5	5	3
MSL ID: 2093	0.0073	0.0111	0.0072	0.2535	0.0078	0.0116	0.0077	0.0074	10	50	5	5	1
MSL ID: 2171	0.0081	0.0152	0.0081	0.5441	0.0096	0.0150	0.0096	0.0082	10	50	50	5	1
MSL ID: 638	0.0111	0.0148	0.0111	0.0259	0.0118	0.0142	0.0118	0.0107	50	50	20	5	3
MSL ID: 913	0.0093	0.0112	0.0093	0.0201	0.0097	0.0109	0.0097	0.0089	15	50	50	5	4
S&P 500 Futures	0.1375	0.1447	0.1375	0.0171	0.1447	0.1375	0.1447	0.0095	50	50	50	5	4
NQ 100 Futures	0.1691	0.1888	0.1691	0.0161	0.1888	0.1691	0.1888	0.0107	5	50	5	5	3
Dow 30	0.1356	0.1456	0.1356	0.0190	0.1456	0.1356	0.1456	0.0087	10	40	10	15	2
Russell 2000	0.1499	0.1769	0.1499	0.0218	0.1769	0.1500	0.1769	0.0121	5	50	50	5	1
DAX	0.1597	0.1728	0.1597	0.0153	0.1728	0.1597	0.1728	0.0068	50	10	5	5	3
CAC 40	0.0901	0.0994	0.0901	0.0186	0.0993	0.0902	0.0993	0.0127	15	40	5	5	2
FTSE 100	0.1238	0.1330	0.1238	0.0174	0.1329	0.1239	0.1329	0.0076	5	10	5	5	2
DJ Euro Stoxx 50	0.0840	0.0907	0.0840	0.0188	0.0905	0.0842	0.0905	0.0098	40	10	5	5	2
FTSE MIB	0.1154	0.1321	0.1154	0.0524	0.1321	0.1155	0.1321	0.0109	5	50	5	5	3
SMI	0.1106	0.1318	0.1106	0.0175	0.1319	0.1106	0.1319	0.0076	5	30	50	5	2
IBEX 35	0.1092	0.1252	0.1092	0.0474	0.1251	0.1093	0.1251	0.0107	50	50	50	5	3
WIG20	0.0613	0.0599	0.0613	0.0246	0.0598	0.0614	0.0598	0.0095	5	50	20	5	4
BUX	0.0896	0.0995	0.0896	0.0210	0.0995	0.0897	0.0995	0.0094	20	50	30	5	1
OBX	0.1271	0.1473	0.1271	0.0202	0.1473	0.1271	0.1473	0.0148	20	50	5	5	1
iBovespa	0.0674	0.0728	0.0674	0.0421	0.0727	0.0675	0.0727	0.0115	5	50	5	5	1
IPC	0.0894	0.1043	0.0894	0.0228	0.1040	0.0896	0.1040	0.0099	50	10	50	5	1
BIST 30	0.0839	0.0946	0.0839	0.0484	0.0945	0.0840	0.0945	0.0142	50	50	50	5	3
Hang Sengs	0.0671	0.0733	0.0671	0.0286	0.0730	0.0674	0.0730	0.0098	50	10	50	5	4
China H-Shares	0.0822	0.0905	0.0822	0.0232	0.0905	0.0823	0.0905	0.0109	5	50	5	5	1
Singapore MSCI	0.1036	0.1025	0.1036	0.0207	0.1024	0.1036	0.1024	0.0095	5	50	5	5	1
BSE Sensex 30	0.1172	0.1352	0.1172	0.0704	0.1359	0.1174	0.1359	0.0697	50	10	40	5	3

Table A3 continued

NITFY	0.1321	0.1446	0.1321	0.0321	0.1455	0.1323	0.1455	0.0094	20	10	5	5	1
KOSPI 200	0.0600	0.0625	0.0600	0.0290	0.0622	0.0602	0.0622	0.0086	5	50	5	5	
Nikkei 225	0.1547	0.1723	0.1547	0.0165	0.1723	0.1548	0.1723	0.0110	30	50	5	5	3
US Dollar Index	0.0423	0.0434	0.0423	0.0193	0.0433	0.0424	0.0433	0.0047	5	40	5	5	3
EUR/USD	0.0841	0.0875	0.0841	0.0144	0.0875	0.0841	0.0875	0.0047	5	40	15	5	2
US 30Y T-Bond	0.0638	0.0753	0.0638	0.0169	0.0749	0.0641	0.0749	0.0069	50	10	50	5	1
Euro Bund	0.0720	0.0850	0.0720	0.0262	0.0850	0.0721	0.0850	0.0052	5	50	5	5	1
Japan Govt. Bond	0.0179	0.0208	0.0179	0.0308	0.0203	0.0183	0.0203	0.0018	20	40	5	5	2
Crude Oil	0.1327	0.1339	0.1327	0.0172	0.1338	0.1327	0.1338	0.0099	5	50	5	5	4
Natural Gas	0.1499	0.1611	0.1499	0.0181	0.1612	0.1499	0.1612	0.0101	50	50	50	5	4
Gold	0.1821	0.2098	0.1821	0.0198	0.2097	0.1821	0.2097	0.0136	50	10	50	5	3
Copper	0.1299	0.1355	0.1299	0.0194	0.1354	0.1299	0.1354	0.0114	40	10	5	5	1
US-Wheat	0.1192	0.1323	0.1192	0.0252	0.1323	0.1192	0.1323	0.0123	50	40	50	5	4

Table A4. Obtained RMSEs in time series datasets by analyzing according to time orders and optimum network parameters.

Datasets	Training RMSE				Test RMSE				Optimum # hidden neurons				Delay
	RNN	RVFL	ANN	R-RVFL	RNN	RVFL	ANN	R-RVFL	RNN	RVFL	ANN	R-RVFL	
SS. ID: 722255	0.1017	0.1140	0.1029	0.0224	0.1063	0.1102	0.1073	0.0235	40	30	50	20	1
SS. ID: 722700	0.0995	0.1137	0.1008	0.0214	0.1040	0.1099	0.1052	0.0229	40	30	50	15	3
SS. ID: 744860	0.1920	0.1424	0.1920	0.0812	0.1362	0.1946	0.1362	0.0287	10	50	15	15	3
SS. ID: 911900	0.0649	0.0876	0.0682	0.0176	0.0684	0.0846	0.0714	0.0191	40	50	40	20	3
MSL ID: 1111	0.0068	0.0110	0.0068	0.0474	0.0086	0.0092	0.0086	0.0064	10	50	10	5	4
MSL ID: 1391	0.0378	0.0471	0.0378	0.0360	0.0411	0.0406	0.0411	0.0327	10	15	15	5	3
MSL ID: 1673	0.0082	0.0153	0.0082	0.0241	0.0094	0.0147	0.0094	0.0077	10	50	10	5	2
MSL ID: 2093	0.0057	0.0125	0.0056	0.0056	0.0085	0.0114	0.0085	0.0084	10	50	5	5	0
MSL ID: 2171	0.0079	0.0205	0.0077	0.0079	0.0092	0.0160	0.0092	0.0098	5	50	5	5	0
MSL ID: 638	0.0116	0.0159	0.0115	0.0378	0.0103	0.0161	0.0105	0.0100	10	50	40	5	3
MSL ID: 913	0.0092	0.0117	0.0091	0.0245	0.0093	0.0107	0.0093	0.0090	5	50	15	5	4
S&P 500 Futures	0.0983	0.0917	0.0983	0.0160	0.0917	0.0984	0.0917	0.0057	20	40	10	5	4
NQ 100 Futures	0.0720	0.1340	0.0720	0.0104	0.1338	0.0720	0.1338	0.0054	5	40	30	5	3
Dow 30	0.1000	0.1123	0.1000	0.0227	0.1121	0.1000	0.1121	0.0057	15	50	50	5	1
Russell 2000	0.0810	0.1624	0.0810	0.0173	0.1621	0.0811	0.1621	0.0072	5	50	5	5	
DAX	0.1211	0.1518	0.1211	0.0103	0.1517	0.1211	0.1517	0.0083	50	40	5	5	3
CAC 40	0.0729	0.0973	0.0729	0.3018	0.0972	0.0730	0.0972	0.0088	5	50	40	5	3
FTSE 100	0.1179	0.1281	0.1179	0.0179	0.1280	0.1179	0.1280	0.0098	5	40	5	10	4
DJ Euro Stoxx 50	0.0677	0.1021	0.0677	0.0204	0.1022	0.0678	0.1022	0.0087	10	50	5	5	3
FTSE MIB	0.1263	0.1324	0.1263	0.1617	0.1326	0.1264	0.1326	0.0093	15	50	5	5	3
SMI	0.0549	0.1138	0.0549	0.1710	0.1138	0.0550	0.1138	0.0070	5	50	5	5	3
IBEX 35	0.1134	0.1208	0.1134	0.0335	0.1210	0.1134	0.1210	0.0083	40	50	5	5	4
WIG20	0.0746	0.0547	0.0746	0.1748	0.0548	0.0746	0.0548	0.0078	15	50	5	5	3
BUX	0.0950	0.1003	0.0950	0.1183	0.1008	0.0951	0.1008	0.0071	5	50	40	5	3
OBX	0.0684	0.1263	0.0684	0.2246	0.1259	0.0685	0.1259	0.0074	5	50	10	5	3
iBovespa	0.0697	0.0718	0.0697	0.3114	0.0722	0.0698	0.0722	0.0119	5	50	30	5	3
IPC	0.0714	0.1079	0.0714	0.0240	0.1074	0.0715	0.1074	0.0074	5	50	5	5	4
BIST 30	0.0830	0.0685	0.0830	0.0229	0.0689	0.0831	0.0689	0.0111	10	50	5	5	3
Hang Sengs	0.0670	0.0648	0.0670	0.0207	0.0647	0.0671	0.0647	0.0079	5	50	10	5	3
China H-Shares	0.0863	0.0919	0.0863	0.2001	0.0923	0.0864	0.0923	0.0086	10	50	5	5	3
Singapore MSCI	0.1357	0.0387	0.1357	0.0214	0.0385	0.1358	0.0385	0.0059	5	50	30	15	1
BSE Sensex 30	0.0565	0.1096	0.0565	0.0838	0.1090	0.0568	0.1090	0.0103	30	50	5	5	3

Table A4. continued

NITFY	0.0563	0.1001	0.0563	0.0430	0.0999	0.0564	0.0999	0.0106	5	50	10	5	3
KOSPI 200	0.0742	0.0456	0.0742	0.0406	0.0451	0.0743	0.0451	0.0078	5	50	30	5	1
Nikkei 225	0.1538	0.1745	0.1538	0.0159	0.1745	0.1538	0.1745	0.0093	50	40	20	10	2
US Dollar Index	0.0412	0.0306	0.0412	0.0515	0.0302	0.0414	0.0302	0.0035	5	40	5	5	1
EUR/USD	0.0963	0.0773	0.0963	0.0310	0.0771	0.0963	0.0771	0.0053	5	40	20	5	3
US 30Y T-Bond	0.0557	0.0646	0.0557	0.0674	0.0641	0.0558	0.0641	0.0045	10	50	15	5	3
Euro Bund	0.0483	0.0797	0.0483	0.0479	0.0791	0.0484	0.0791	0.0033	5	50	5	5	3
Japan Govt. Bond	0.0139	0.0202	0.0139	0.1187	0.0192	0.0145	0.0192	0.0013	15	50	5	5	1
Crude Oil	0.1448	0.0843	0.1448	0.0185	0.0841	0.1448	0.0841	0.0089	5	40	15	5	3
Natural Gas	0.1605	0.1596	0.1605	0.0330	0.1599	0.1605	0.1599	0.0076	5	40	5	5	4
Gold	0.1495	0.2499	0.1495	0.0106	0.2499	0.1495	0.2496	0.0091	5	40	5	5	1
Copper	0.1550	0.1068	0.1550	0.0472	0.1064	0.1550	0.1064	0.0106	5	40	5	5	3
US-Wheat	0.1256	0.0906	0.1256	0.0292	0.0905	0.1256	0.0905	0.0107	10	50	5	5	4